Supplementary data

Amorphous WO_3 Induced Lattice Distortion for a Low-Cost and Highly-Efficient Electrocatalyst for Overall Water Splitting in Acid

Ke Fan[a,d]*, Min He[a], N. V. R. Aditya Dharanipragada[c], Panyong Kuang[a], Yufei Jia[a], Lizhou Fan[b], A. Ken Inge[c], Biaobiao Zhang[b,]*, Licheng Sun[b,d], Jiaguo Yu[a,]*

[a]State Key Laboratory of Advanced Technology for Materials Synthesis and Processing, Wuhan University of Technology, Wuhan 430070, P. R. China

[b]Department of Chemistry, KTH Royal Institute of Technology, 10044 Stockholm, Sweden

[c]Department of Materials and Environmental Chemistry, Stockholm University, 10691 Stockholm, Sweden

[d]State Key Laboratory of Fine Chemicals, Institute of Artificial Photosynthesis, DUT−KTH Joint Education and Research Center on Molecular Devices, Institute for Energy Science and Technology, Dalian University of Technology (DUT), 116024 Dalian, P. R. China

Tel: 0086-27-87871029, Fax: 0086-27-87879468

E-mail: jiaguoyu@yahoo.com; kefan@kth.se; biaobiao@kth.se

Experimental section

Chemicals and Materials

Aniline ($C_6H_7N_2$, JIS Special Grade), nitric acid (HNO_3, JIS Special Grade), sulfuric acid (H_2SO_4, JIS Special Grade), iridium chloride hydrate ($IrCl_3 \cdot xH_2O$, 99.99% metals basis, Ir ≥ 63.9%), iridium oxide (IrO_2, 99.9% metals basis, Ir ≥ 84.5%) and tungsten chloride (WCl_6, 99%) was purchased from Aladdin. 20% Pt/C was purchased from WingRise. Carbon paper (CP) was provided by Toray (Japan).

Synthesis of catalysts

The preparation of hierarchical PANI nanofibers was achieved *via* the electrodeposition method using a three-electrode system. CP (2 × 2 cm^2) was firstly treated at 550 ℃ in air for 3 h and immersed in concentrated nitric acid for 10 minutes. The treated CP was used as the working electrode and counter electrode, and saturated calomel electrode (SCE) was used as the reference electrode. The electrolyte was prepared by dissolving 7.4 mL concentrated HNO_3 in 88 mL H_2O and then adding 4.6 mL aniline to form uniform solution after stirring for 1 h. The *in situ* electrodeposition was carried out at a current density of 2 mA cm^{-2} for 1200 s on CP electrode. After that, PANI/CP was washed with water and repeated the above operation again, followed by drying at 80 ℃ for 1 h. The redox states of PANI were tailored by the potentiostatic method. The samples were treated at 0 V (*vs*. SCE) for 0.5 h and then immersed in 50 mL water for 30 min. Next, metal complex solution was prepared by dissolving $IrCl_3 \cdot xH_2O$ and WCl_6 in 80 mL H_2O (Ir + W = 0.1 M) and the treated PANI was directly immersed in the solution for 1 h under stirring. After a full cation exchange reaction, the obtained $Ir_{1-x}W_x$/PANI hybrids were washed three times and dried in vacuum at 60 ℃ for 1 h. Finally, the hybrid precursor was carbonized at 900 ℃ in N_2 atmosphere for 3 h (this process transformed PANI to N-doped carbon material (NC)). The obtained samples were termed as $Ir_{1-x}W_x$@NC. The mass loading of Ir/W is determined by the inductively coupled plasma-atomic emission spectroscopy (ICP-AES). In order to demonstrate the effect of iridium and tungsten

content on the catalytic activity, the mole ratio of iridium to tungsten in the initial solution was varied while the sum Ir + W = 0.1 M was kept (Ir/W = 1/0, 9/1, 5/5, 1/9, 0/1 and blank PANI after carbonization, denoted as Ir@NC, $Ir_{0.9}W_{0.1}$@NC, $Ir_{0.5}W_{0.5}$@NC, $Ir_{0.1}W_{0.9}$@NC, W@NC and NC, respectively) to prepare different samples in the same procedure.

Materials characterization

The morphology was observed with field emission scanning electron microscopy (FE-SEM, JEOL JSM-7500) operated at 5 kV. Powder X-ray diffraction (XRD) was performed on a Rigaku diffractometer (Japan) with monochromated Cu Kα radiation (40 kV, 40 mA). Inductively coupled plasma atomic emission spectroscopy (ICP-AES) measurements were performed on Prodigy 7/Prodigy 7. Transmission electron microscopy (TEM), high resolution transmission electron microscopy (HR-TEM), high-Angle annular dark field-scanning transmission electron microscopy (HAADF-STEM) images, selected area electron diffraction (SAED), energy-dispersive X-ray spectroscopy (EDXS), and elemental mapping analysis were performed using a JEM-ARM300F operated at 200 kV. Raman spectroscopy was performed using RenishawinVia spectrometer (λ = 630 nm) at room temperature. X-ray photoelectronic spectroscopy (XPS) spectra were carried out by using a Thermo ESCALAB 250XI instrument with an Al Kα X-ray source.

Electrochemical measurements

The electrochemical performance of the as-prepared catalysts was evaluated in a three-electrode system by using an electrochemical workstation (CHI 660E, Chenhua Shanghai) in 0.5 M H_2SO_4 as the electrolyte. The as-prepared electrodes, saturated silver chloride electrode (saturated KCl, Ag/AgCl), Pt foil (for OER) and graphite plate (for HER) were used as working, reference and counter electrode, respectively. The effective working area of the as-prepared electrodes was 1 cm^2. The linear sweep voltammetry (LSV) curves of Ir_xW_{1-x}@NC electrodes were carried out at a scan rate of 5 mV s^{-1} for OER, HER and overall water splitting. The chronopotentiometric

curves of electrodes were tested at given current densities. The electrochemical impedance spectroscopy (EIS) measurements were conducted at fixed overpotential of 300 mV for OER with the frequency range of 0.1 Hz to 100 kHz (10 mV amplitude).

In this work, all potentials measured were calibrated to *vs*. reversible hydrogen electrode (RHE):

E (RHE) =E (Ag/AgCl) + 0.197 V + 0.059 × pH.

All the electrochemical data were recorded with iR compensation unless otherwise stated.

Turnover frequency (TOF) measurements

Turnover frequency (TOF) was determined as the number of catalytic reaction conversions occurring per active site per time. WO_3 is a very kinetically sluggish for OER. Thus in the hybrid IrW@NC catalyst, the Ir cation sites are presumed to support the large majority of oxygen evolution turnover. An Ir-specific turnover frequency was thus calculated to highlight the activity of the Ir sites accounting for their fraction of the total metal cations, assuming 100% reaction at Ir sites, and then, the TOF (s^{-1}) were calculated with the following equation: TOF = I/(4nF), where I is the catalytic current (A), F is the Faraday constant (96485 C mol^{-1}), n is the number of active sites (mol). TOF was evaluated at an overpotential of 300 mV according to the reported method. For HER, the TOF was calculated with the following equation: TOF = I/(2nF), which was evaluated at an overpotential of 100 mV.

XAS Data Analysis

The XAS spectra were measured at the beamline P64, PETRA III, DESY, Hamburg. The data was acquired in transmission mode by measuring the sample and reference W foil simultaneously. The analysis was carried out using EXAFS PAK including the data refinement steps of pre-edge and post-edge background removal and normalization. The k^3-weighted EXAFS oscillations were analyzed by nonlinear least-squares fits of the data to the EXAFS equation. The various model parameters:

average coordination number (N), mean interatomic distances (R), Debye–Waller factor coefficients (σ^2), and threshold energy (E_0) were refined. Fourier transformation and data fitting were performed using the EXAFS PAK data package. The theoretical phases and amplitudes used in the refinements were calculated using FEFF7.[1]

The EXAFS data were modelled using the FEFF7 generated paths based on a distorted WO_6 octahedral model. The reference was modelled in accordance with the geometry of WO_3 by fixing the first shell coordination number and refining the radial distance as well as Debye-Waller factor. The second shell was modelled using W-O and W-O-W multiple scattering contributions and was refined for radial distance and Debye-Waller factor. The structural fitting of the sample $Ir_{0.5}W_{0.5}$@NC was performed by refining the Debye-Waller factor, coordination number and radial distance of the first as well as second shell contributions. The first shell structure was refined using a W-O single scattering path. Similar multiple scattering paths (W-O, W-O-W) as that of reference WO_3 were used to fit the second shell. An additional W-O-Ir distance was necessary to obtain a best fit. The results are documented in Table S2.

Table S1. The content of Ir and W in the final materials according to the ICP test.

Catalyst	Ir Content (mg/g)	W Content (mg/g)	Initial molar ratio in solution (Ir/W)	Final molar ratio in material (Ir/W)
Ir@NC	0.81	0	-	-
$Ir_{0.9}W_{0.1}$@NC	0.71	1.65	9	0.43
$Ir_{0.5}W_{0.5}$@NC	0.51	2.15	1	0.19
$Ir_{0.1}W_{0.9}$@NC	0.29	3.69	0.11	0.08
W@NC	0	3.95	0	0

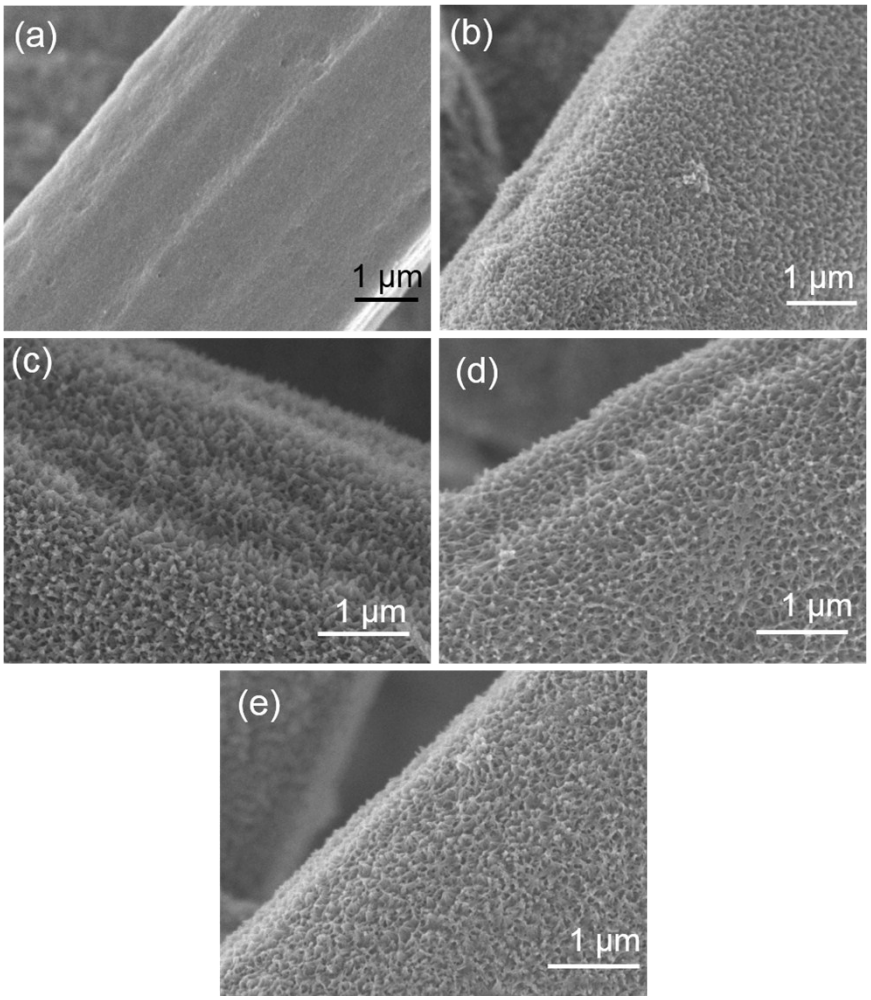

Figure S1. SEM images of (a) the bare CP, (b) PANI on CP, (c) Ir@NC, (d) $Ir_{0.5}W_{0.5}$@NC, and (e) W@NC.

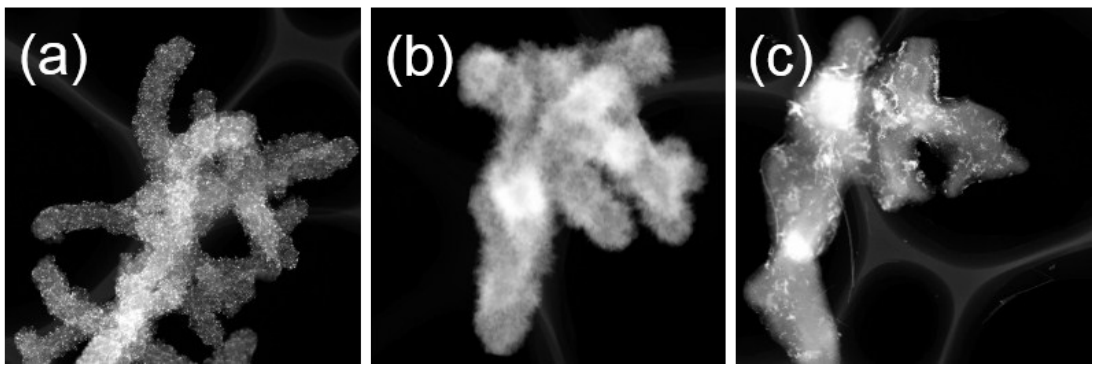

Figure S2. High-angle annular dark field images of (a) Ir@NC, (b) W@NC and (c) $Ir_{0.5}W_{0.5}$@NC.

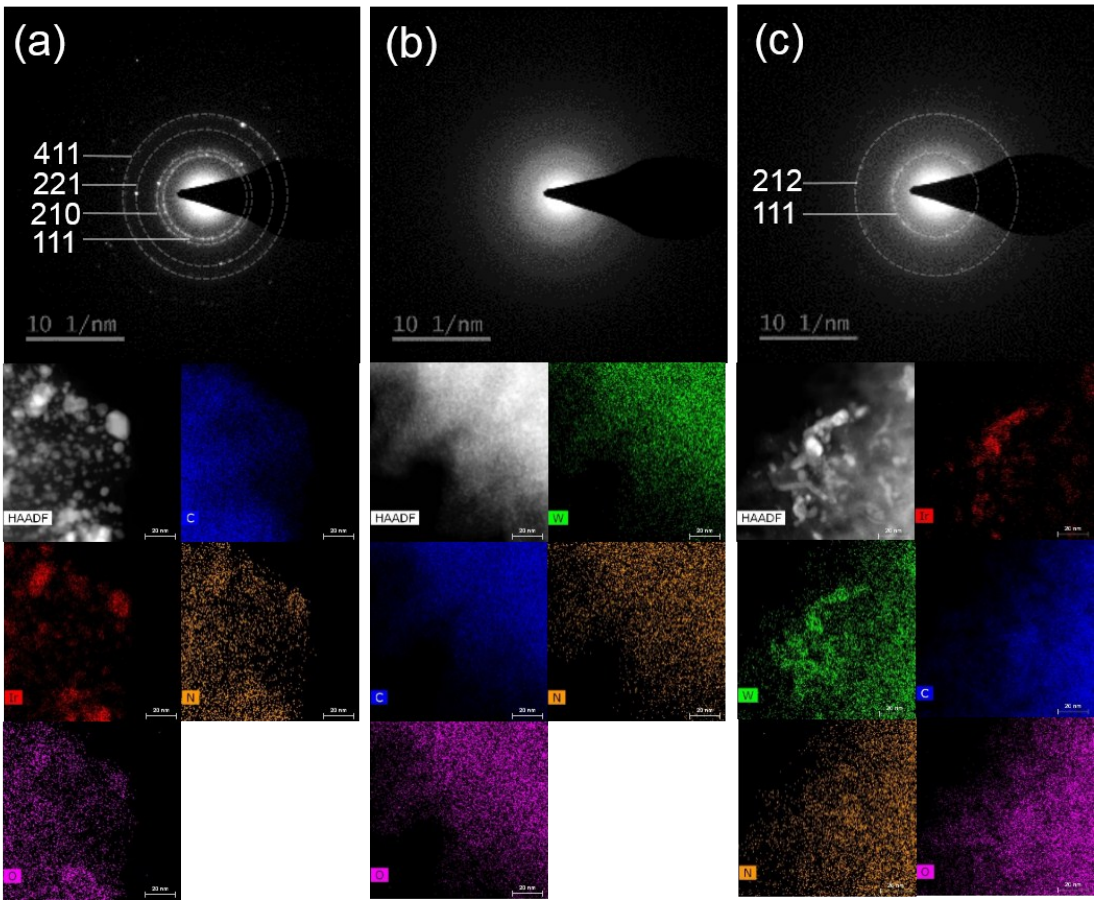

Figure S3. SAED and EDS mapping images of (a) Ir@NC, (b) W@NC and (c) $Ir_{0.5}W_{0.5}$@NC.

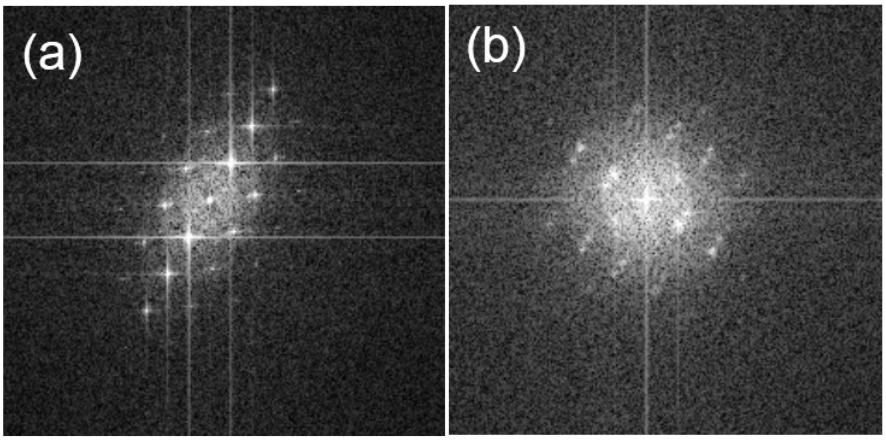

Figure S4. FFT patterns of (a) Ir@NC and (b) $Ir_{0.5}W_{0.5}$@NC

Table S2: The results of the structural parameters of the reference WO_3 and $Ir_{0.5}W_{0.5}$@NC obtained by fitting of EXAFS spectra.

	WO_3			$Ir_{0.5}W_{0.5}$@NC		
	N[a]	**R[b]**	**σ^{2a}**	**N[a]**	**R[b]**	**$\sigma^{2\,a}$**
W-O	6	1.70(3)	0.005(4)	5.2	1.81(6)	0.008(7)
W-O*	4	2.56(5)	0.005(3)	3.5	2.56(5)	0.005(5)
W-O-M	2	3.31(2)	0.019(2)	1.8	3.1(2)	00.019(7)
W-O-Ir(M)	–	–	–	2.1	3.3(3)	0.0028(8)

*W-O multiple scattering contribution. [a]The estimated error of the CN values is ca. 25%. [b]The standard deviations in parentheses were obtained from k^3-weighted least-squares refinements of the EXAFS function $\chi(k)$ and do not include systematic errors of the measurement.

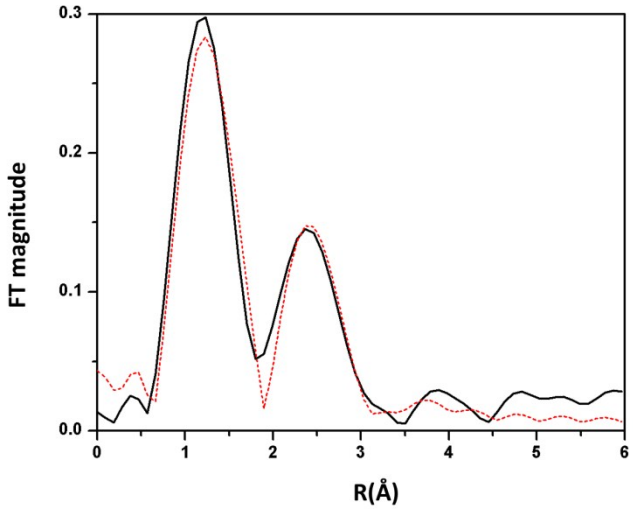

Figure S5. Fit of the W-L_3 edge Fourier transform of $Ir_{0.5}W_{0.5}$@NC. The Fourier transformed EXAFS spectra are without phase corrections for the experimental data. Black solid line: data, red dotted line: fit.

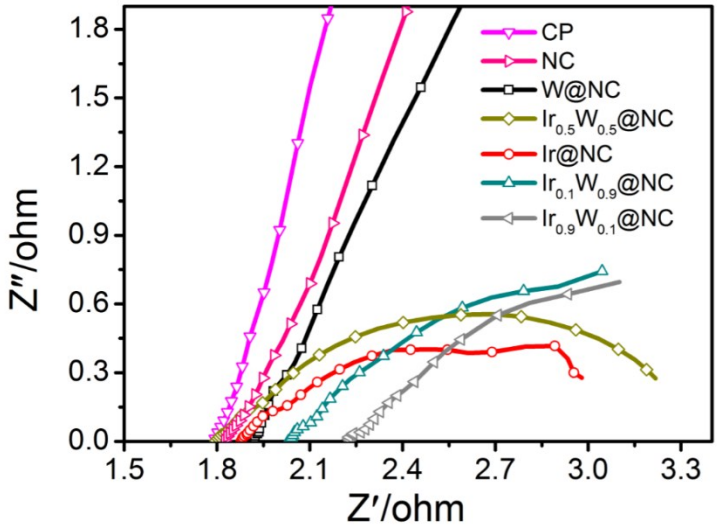

Figure S6. Nyquist plots at the overpotential of 300 mV for OER in 0.5 M H_2SO_4

Table S3. TOFs of the reported state-of-the-art catalysts containing noble metals in acid medium for OER.

Catalyst	Noble metal loading (mg cm^{-2})	Electrolyte	TOF (s^{-1}) @η = 0.3 V	Ref.
$Ir_{0.5}W_{0.5}$@NC	**0.005**	**0.5 M H_2SO_4**	**2.07**	**This work**
$IrNi_x/IrO_2$	0.01	0.05 M H_2SO_4	1.29	***Angew. Chem.*** 2015, 3, 3018-3022
Pd@Ir_{4L}	0.075	0.1 M $HClO_4$	0.4	***Angew. Chem.*** 2019, 5, 7244-7248
$W_{0.99}Ir_{0.01}O_{3-\delta}$	0.11	1 M H_2SO_4	1.3	***Energy Environ. Sci.*** 2017, 10, 2432
$IrNi_{0.57}W_{0.82}$	0.09	0.5 M $HClO_4$	0.56	***J. Mater. Chem. A*** 2017, 5, 24836-24841
IrCoNi	0.05	0.5 M H_2SO_4	0.26	***Adv. Mater.*** 2017, 12, 1703798
NPC@RuO_2	0.357	0.1 M $HClO_4$	0.4	***Adv. Funct. Mater.*** 2019, 4, 1901154
Li-IrO_x	0.05	0.5 M H_2SO_4	0.3	***J. Am. Chem. Soc.*** 2019, 2, 3014-3023

References

[1] a) J. J. Rehr, J. J. Kas, M. P. Prange, A. P. Sorini, Y. Takimoto, F. Vila, *Comptes Rendus Physique* **2009**, *10*, 548-559; b) S. Zabinsky, J. Rehr, A. Ankudinov, R. Albers, M. Eller, *Physical Review B* **1995**, *52*, 2995.